Cosmological consequences of the model of low-energy quantum gravity

Michael A. Ivanov

Physics Dept.,

Belarus State University of Informatics and Radioelectronics,
6 P. Brovka Street, BY 220027, Minsk, Republic of Belarus.
E-mail: ivanovma@tut.by.

April 17, 2016

Abstract

The model of low-energy quantum gravity by the author is based on the conjecture about an existence of the graviton background. An interaction of photons and moving bodies with this background leads to small additional effects having essential cosmological consequences. In the model, redshifts of remote objects and the dimming of supernovae 1a may be interpreted without any expansion of the Universe and without dark energy. Some of these consequences are discussed and confronted with supernovae 1a, long GRBs, and QSOs observations in this paper. It is shown that the two-parametric theoretical luminosity distance of the model fits observations with high confidence levels (100% for the SCP Union 2.1, 43% for JLA compilations, 99.81% for long GRBs, and 13.73% for quasars), if all data sets are corrected for no time dilation. These two parameters are computable in the model.

$PACS$: 98.80.Es, 04.50.Kd, 04.60.Bc

1 Introduction

In contrast with classical electrodynamics in the XIX century or quantum electrodynamics in the XX century, at present we have a complete lack of experimental evidence to construct a theory of quantum gravity. From dimensional reasons only, if one assumes that the Newton constant is universal for any scales, the effects of quantum gravity are expected to be measurable over extremely small distances or very high energies. There are proposals how to detect some effects in a laboratory - for example, [1, 2], - or to observe a possible small violation of the Lorentz invariance for remote sources, but we have not any results in a frame of current paradigms which may pave us to the goal. Another constrain is, as I think, the common expectation that the future theory should be some

symbiosis of the geometrical theory of general relativity and quantum mechanics. Geometry is useful for a description of the average motion of big bodies due to the universality of gravitation, but it is not the fact that quantum effects may be described geometrically. It is also necessary to keep in mind that the nature of gravity as well as the nature of quantum behavior of microparticles are unknown - we have remarkable descriptions in different languages but not understanding in both cases.

I describe here briefly some consequences of my approach to quantum gravity [3, 4], in which the phenomenon is a very-low-energy one and is caused by the background of super-strong interacting gravitons. The main quantum effect of this approach is the Newtonian attraction; its small effects enforce us to look at the known results of astrophysical observations from another point of view and give us the reasons to doubt in the validity of the current standard cosmological model.

2   The model of low-energy quantum gravity

The geometrical description of gravity in general relativity does not involve any mechanism of interaction. It is similar to the Newtonian model: we don't know how it works. In my model of low-energy quantum gravity [3, 4], gravity is considered as the screening effect. It is suggested that the background of super-strong interacting gravitons exists in the universe. Its temperature should be equal to the one of CMB. Screening this background creates for any pair of bodies both attraction and repulsion forces due to pressure of gravitons. For single gravitons, these forces are approximately balanced, but each of them is much bigger than a force of Newtonian attraction. If single gravitons are pairing, an attraction force due to pressure of such graviton pairs is twice exceeding a corresponding repulsion force if graviton pairs are destructed by collisions with a body. This peculiarity of the quantum mechanism of gravity leads to the difference of inertial and gravitational masses of a black hole. In such the model, the Newton constant is connected with the Hubble constant that gives a possibility to obtain a theoretical estimate of the last. We deal here with a flat non-expanding universe fulfilled with super-strong interacting gravitons; it changes the meaning of the Hubble constant which describes magnitudes of three small effects of quantum gravity but not any expansion or an age of the universe.

3   Small effects of the model due to its quantum nature

There are two small effects for photons in the sea of super-strong interacting gravitons [3]: average energy losses of a photon due to forehead collisions with gravitons and an additional relaxation of a photonic flux due to non-forehead collisions of photons with gravitons. The first effect leads to the geometrical

distance/redshift relation:

$$r(z) = ln(1 + z) \cdot c/H_0, \qquad (1)$$

where H_0 is the Hubble constant, c is the velocity of light. The both effects lead to the luminosity distance/redshift relation:

$$D_L(z) = c/H_0 \cdot \ln(1 + z) \cdot (1 + z)^{(1+b)/2} \equiv c/H_0 \cdot f_1(z), \qquad (2)$$

where $f_1(z) \equiv \ln(1+z) \cdot (1+z)^{(1+b)/2}$; the "constant" b belongs to the range 0 - 2.137 [5] ($b = 2.137$ for very soft radiation, and $b \rightarrow 0$ for very hard one). For an arbitrary source spectrum, a value of the factor b should be still computed. It is clear that in a general case it should depend on a rest-frame spectrum and on a redshift. Because of this, the Hubble diagram should be a multivalued function of a redshift: for a given z, b may have different values for different kinds of sources. Further more, the Hubble diagram may depend on the used procedure of observations: different parts of rest-frame spectrum will be characterized with different values of the parameter b.

Actually, the factor b describes an analog of the blurring effect of tired-light models. Due to the quantum nature of this effect in the model, non-forehead collisions of photons with gravitons should lead to relatively big average angles of deviations of photons of visible range:

$$\Delta\varphi \sim \frac{10^{-3} \ eV}{2.5 \ eV} = 4 \cdot 10^{-4} \ rad,$$

where $10^{-3} \ eV$ and 2.5 eV are average graviton and photon energies. By multiple collisions, deviated photons will not be recognized as emitted by a small-angle remote object. But images of high-z objects may be partly blurred due to a fraction of low-energy gravitons.

The third small effect of this model is the constant deceleration of massive bodies due to forehead collisions with gravitons. It is an analog of the redshift in this model. We get for the body acceleration w by a non-zero velocity v:

$$w = -ac^2(1 - v^2/c^2). \qquad (3)$$

For small velocities we have for it: $w \simeq -H_0 c$. If the Hubble constant H_0 is equal to $2.14 \cdot 10^{-18} s^{-1}$ (it is the theoretical estimate of H_0 in this approach), a modulus of the acceleration will be equal to $|w| \simeq H_0 c = 6.419 \cdot 10^{-10} \ m/s^2$, that is of the same order of magnitude as a value of the observed additional acceleration $(8.74 \pm 1.33) \cdot 10^{-10} m/s^2$ for NASA probes Pioneer 10/11 [6].

4 Advanced $LIGO$ technologies may be partly used to verify the redshift mechanism

The main conjecture of this approach about the quantum gravitational nature of redshifts may be verified in a ground-based laser experiment. To do it, one
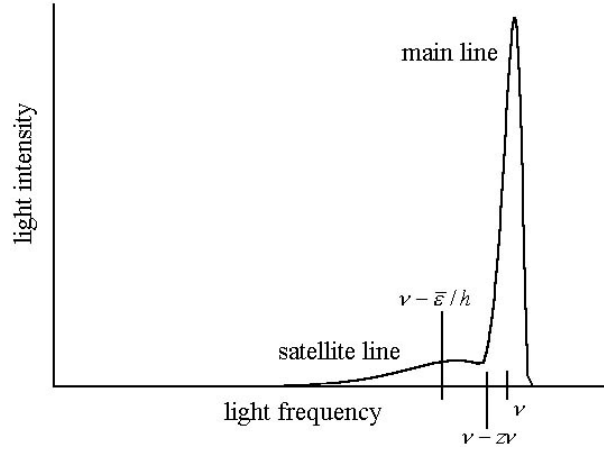
Figure 1: The main line and the expected red-shifted satellite line of a stable laser radiation spectrum after a delay line. Satellite's position should be fixed near $\nu - \bar{\epsilon}/h$, and its intensity should linear rise with a path of photons in a delay line, l. A center-of-mass of both lines is expected to be approximately near $\nu - z\nu$.

should compare spectra of laser radiation before and after passing some distance l in a high-vacuum tube [7]. The temperature T of the graviton background coincides in the model with the one of CMB. Assuming $T = 2.7K$, we have for the average graviton energy: $\bar{\epsilon} = 8.98$ eV. Because of the quantum nature of redshift, the satellite of main laser line of frequency ν would appear after passing the tube with a redshift of 10^{-3} eV/h, and its position should be fixed (see Fig. 1, z is the redshift). It will be caused by the fact that on a very small way in the tube only a small part of photons may collide with gravitons of the background. The rest of them will have unchanged energies. The center-of-mass of laser radiation spectrum should be shifted proportionally to a photon path. Due to the quantum nature of shifting process, the ratio of satellite's intensity to main line's intensity should have the order: $\sim \frac{h\nu}{\bar{\epsilon}} \frac{H_0}{c} l$,. The theoretical value of H_0 in the model is: $H_0 = 2.14 \cdot 10^{-18}$ s^{-1}. An instability of a laser must be only much smaller than 10^{-3} if a photon energy is equal to ~ 1 eV. Given a very low signal photon number frequency, one could use a single photon counter to measure the intensity of the satellite line after a narrow-band filter with filter transmittance k. If q is a quantum output of a photomultiplier cathode, f_n is a frequency of its noise pulses, and n is a desired signal-to-noise ratio, then an evaluated time duration t of data acquisition would be equal to:

$$t = \frac{(\bar{\epsilon}cn)^2 f_n}{(H_0 qkPl)^2},$$

where P is a laser power. Assuming for example: $n = 10$, $f_n = 10^3$ s^{-1}, $q = 0.3$, $k = 0.1$, $P = 200$ W, $l = 300$ km, we have the estimate: $t \approx 3 \cdot 10^3$ s. Such the

4

value of l may be achieved if one forces a laser beam to whipsaw many times between mirrors in the vacuum tube with the length of a few kilometers.
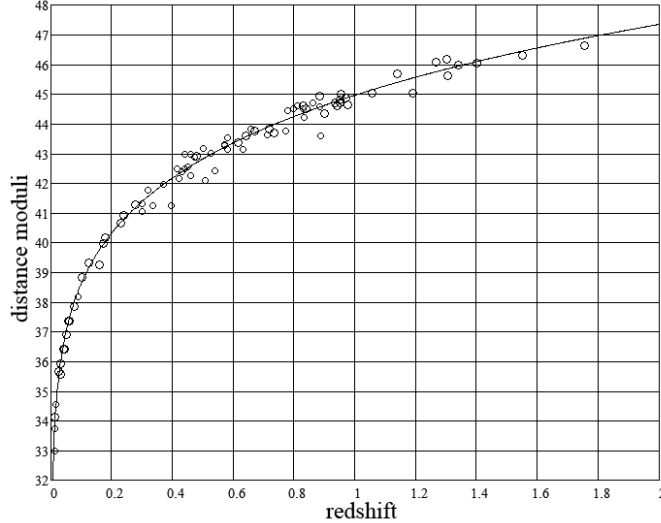

Figure 2: The theoretical Hubble diagram $\mu_0(z)$ of this model (solid); Supernovae 1a observational data (circles, 82 points) are taken from Table 5 of [12] and corrected for no time dilation.

The advanced $LIGO$ detectors [8], which were used to observe the gravitational-wave event $GW150914$, have many technological achievements needed to do the described experiment: stable powerful lasers and input optics, high-vacuum tubes with optical resonator that multiplies the physical length by the number of round-trips of the light, mirror suspension systems with actuators. Some parameters of $LIGO$ systems are of the same order as in the considered example. If one constructs the future $LIGO$ detector with some additional equipment, the verification of the redshift mechanism may be performed in parallel with the main task or during a calibration stage of the detector.

5 Cosmological consequences of the model

There are the two circumstances introduced in the model to rich the needed strength of gravitational attraction: 1) gravitons should be super-strong interacting, and 2) a part of gravitons should be paired and the pairs must be destructed by interaction with bodies. It leads to the very unexpected consequence: in the model, a black hole should have different gravitational and inertial masses, i. e. its possible existence contradicts to general relativity. Another unexpected feature of this approach is a necessity of "an atomic structure" of matter, because the considered mechanism doesn't work without it.
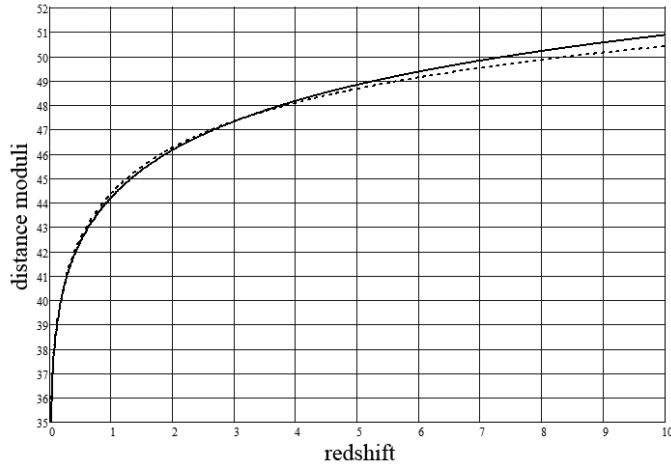
Figure 3: The two theoretical Hubble diagrams: $\mu_0(z)$ of this model with $b = 1.137$ taking into account the effect of time dilation of the standard model (solid); $\mu_c(z)$ for a flat Universe with the concordance cosmology by $\Omega_M = 0.27$ and $w = -1$ (dash).

The property of asymptotic freedom of this model at very short distances leads to the important consequences, too. First, a black hole mass threshold should exist. A full mass of black hole should be restricted from the bottom with m_0; the rough estimate for it is: $m_0 \sim 10^7 M_\odot$. The range of transition to gravitational asymptotic freedom for a pair of protons is between $10^{-11} - 10^{-13}$ meter, and for a pair of electrons it is between $10^{-13} - 10^{-15}$ meter. This transition is non-universal; it means, second, that a geometrical description of gravity on this or smaller scales, for example on the Planck one, is not valid.

Any massive body moving relative to the graviton background should suffer in the model the constant deceleration of the order of $\sim H_0 c$, i. e. of the same order as an anomalous acceleration of the NASA's deep space probes (the Pioneer anomaly) [6]. Recently, it was shown by S. Turyshev et al [9], that the thermal origin of the Pioneer anomaly is very possible. From another side, the mass discrepancy in spiral galaxies appears at very low accelerations less than some a_0 and not much above a_0 [10], where the boundary acceleration a_0 has the same order. The need for dark matter in spiral galaxies appears at very low accelerations. A simple alternative to dark matter is MOND by M. Milgrom [11], in which such the boundary acceleration is introduced by hand. The main feature of MOND is the strengthening of gravitational attraction in a case of low accelerations; I do not think that an exact form of this strengthening has been guessed in MOND. But MOND gives us a clear hint that general relativity may be not valid on galactic or bigger scales of distances, and its application in cosmology is in doubt. In my model, the universal deceleration of bodies should lead in any bound system to an additional acceleration of them relative to the

system's center of inertia. Some additional strengthening of gravitation on a periphery of galaxies may be caused in the model by the destruction of graviton pairs flying through their central parts whereas pairs flying to the center are destructed in a less degree. The problem is open in this model.
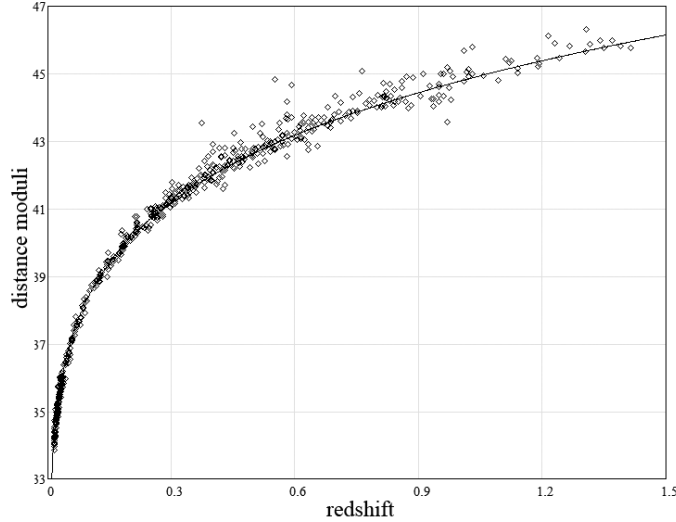

Figure 4: The theoretical Hubble diagram $\mu_0(z)$ of this model (solid); Supernovae 1a observational data (580 points of the SCP Union 2.1 compilation) are taken from [13] and corrected for no time dilation.

The standard cosmological model is based on the assumption that redshifts of remote objects arise due to an expansion of the Universe. The model was rebuilded a few times to save this base, the last innovation of it is an introduction of dark energy. Many people are searching for dark energy now or plan to do it, for example, with the help of big colliders. This basic cosmological assumption is considered by the community as a dogma, an invioalable sanctuary of present cosmology. For example, all observations of remote objects in the time domain are corrected for time dilation - but this effect is an attribute only of the standard model. In my model this assumption does not seem to be absolutely necessary. There exists a possibility in the model to interpret observations in another manner, without any expansion of the Universe.

5.1 The Hubble diagram of this model

In this model, the luminosity distance is given by *Eq.* 2. The theoretical value of relaxation factor b for a soft radiation is $b = 2.137$. Let us begin with this value of b, considering the Hubble constant as a single free parameter to fit observations. The theoretical Hubble diagram of this model is compared with Supernovae 1a observational data by Riess et al. [12] (corrected for no time

dilation as: $\mu(z) \rightarrow \mu(z) + 2.5 \cdot lg(1+z))$ in Fig. 2. As you can see, the theoretical diagram fits observations very well without any dark energy.
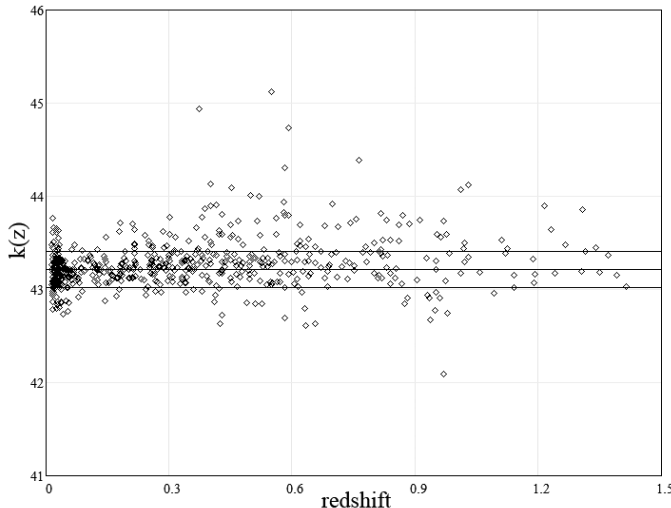

Figure 5: Values of $k(z)$ (580 points) and $< k(z) >$, $< k(z) > +\sigma_k$, $< k(z) > -\sigma_k$ (lines) for the SCP Union 2.1 compilation.

The luminosity distance in the concordance cosmology by $w = -1$ is:

$$D_L(z) = c/H_0 \cdot (1+z) \int_0^z [(1+x)^3 \Omega_M + (1-\Omega_M)]^{-0.5} dx \equiv c/H_0 \cdot f_2(z), \ (4)$$

where $f_2(z) \equiv (1+z) \int_0^z [(1+x)^3 \Omega_M + (1-\Omega_M)]^{-0.5}$, Ω_M is the normalized matter density. To demonstrate how similar are predictions about distance moduli as a function of redshift of this model and of the concordance cosmology, the two theoretical Hubble diagrams are sown in Fig. 3: $\mu_0(z)$ of this model with $b = 1.137$ taking into account the effect of time dilation of the standard model (solid); and $\mu_c(z)$ for a flat Universe with the concordance cosmology by $\Omega_M = 0.27$ and $w = -1$ (dash). You can see a good accordance of this diagrams up to $z \approx 4$.

At present, two big compilations of SN 1a observations are available: the SCP Union 2.1 compilation (580 supernovae) [13] and the JLA compilation (740 supernovae) [14]. These compilations may be used to evaluate the Hubble constant in this approach. Using the definition of distance modulus: $\mu(z) = 5lgD_L(z)(Mpc) + 25$, we get from Eq. 2 for the theoretical distance modulus $\mu_0(z)$: $\mu_0(z) = 5lgf_1(z) + k$, where the constant k is equal to:

$$k \equiv 5lg(c/H_0) + 25.$$

If the model fits observations, then we shall have for $k(z)$:

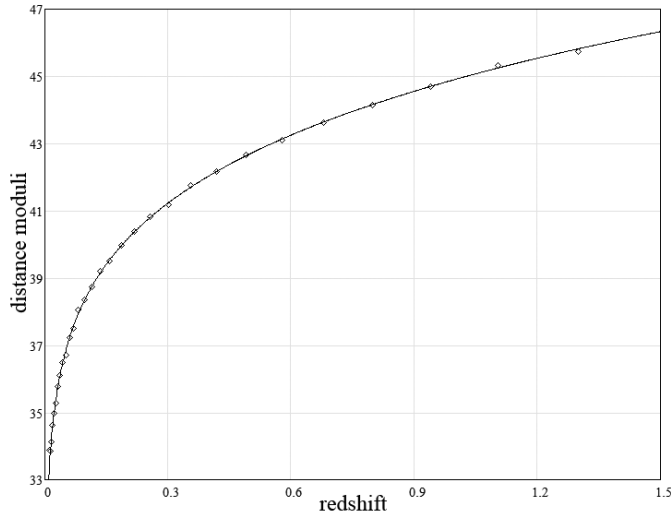$$k(z) = \mu(z) - 5lgf_1(z), \qquad\qquad (5)$$

8

Figure 6: The theoretical Hubble diagram $\mu_0(z)$ of this model with $b = 2.365$ (solid); Supernovae 1a observational data (31 binned points of the JLA compilation) are taken from Tables F.1 and F.2 of [14] and corrected for no time dilation.

where $\mu(z)$ is an observational value of distance modulus. The weighted average value of $k(z)$:

$$< k(z) >= \frac{\sum k(z_i)/\sigma_i^2}{\sum 1/\sigma_i^2}, \tag{6}$$

where σ_i^2 is a dispersion of $\mu(z_i)$, will be the best estimate of k. Here, σ_i^2 is defined as: $\sigma_i^2 = \sigma_{i\ stat}^2 + \sigma_{i\ sys}^2$. The average value of the Hubble constant may be found as:

$$< H_0 >= \frac{c \cdot 10^5}{10^{<k(z)>/5} \cdot Mpc}. \tag{7}$$

For a standard deviation of the Hubble constant we have:

$$\sigma_0 = \frac{ln10 \cdot < H_0 >}{5} \cdot \sigma_k, \tag{8}$$

where σ_k^2 is a weighted dispersion of k, which is calculated with the same weights as $< k(z) >$.

The theoretical Hubble diagram $\mu_0(z)$ of this model with $< k(z) >$ which is calculated using the SCP Union 2.1 compilation [13] is shown in Fig. 4 together with observational points corrected for no time dilation. Values of $k(z)$ (580 points) and $< k(z) >$, $< k(z) > +\sigma_k$, $< k(z) > -\sigma_k$ (lines) are shown in Fig. 5. For this compilation we have: $< k > \pm\sigma_k = 43.216 \pm 0.194$. Calculating the χ^2 value as:

$$\chi^2 = \sum \frac{(k(z_i)- < H_0 >)^2}{\sigma_i^2}, \tag{9}$$

9

we get $\chi^2 = 239.635$. By 579 degrees of freedom of this data set, it means that the hypothesis that $k(z) = const$ cannot be rejected with 100% C.L. Using $Eqs.$ 6, 7, we get for the Hubble constant from the fitting:

$$< H_0 > \pm\sigma_0 = (2.211 \pm 0.198) \cdot 10^{-18} \ s^{-1} = (68.223 \pm 6.097) \frac{km}{s \cdot Mpc}.$$

The theoretical value of the Hubble constant in the model: $H_0 = 2.14 \cdot 10^{-18} \ s^{-1} = 66.875 \ km \cdot s^{-1} \cdot Mpc^{-1}$ belongs to this range. The traditional dimension $km \cdot s^{-1} \cdot Mpc^{-1}$ is not connected here with any expansion.

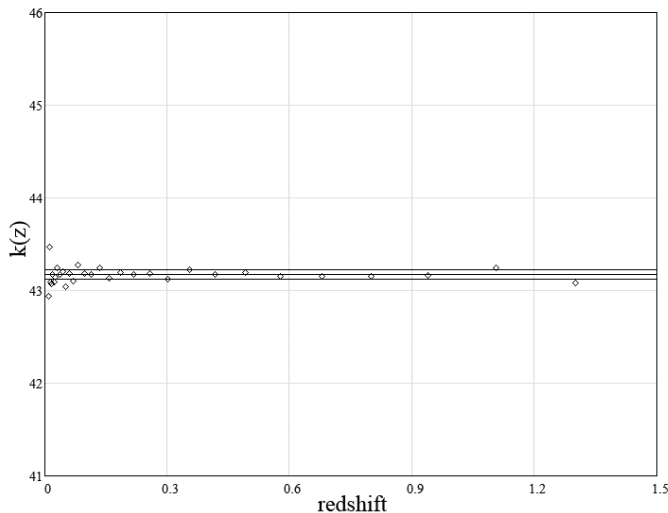Figure 7: Values of $k(z)$ (31 binned points) and $< k(z) >$, $< k(z) > +\sigma_k$, $< k(z) > -\sigma_k$ (lines) for the JLA compilation.

To repeat the above calculations for the JLA compilation, I have used 31 binned points from Tables F.1 and F.2 of [14] (diagonal elements of the correlation matrix in Table F.2 are dispersions of distance moduli). We have for this compilation by $b = 2.137$: $< k > \pm\sigma_k = 43.174 \pm 0.049$ with $\chi^2 = 51.66$. By 30 degrees of freedom of this data set, it means that the hypothesis that $k(z) = const$ cannot be rejected only with 0.83% C.L. Varying the value of b, we find the best fitting value of this parameter: $b = 2.365$ with $\chi^2 = 30.71$. It means that the hypothesis that $k(z) = const$ cannot be rejected now with 43.03% C.L. This value of b is 1.107 times greater than the theoretical one. For the Hubble constant we have in this case:

$$< H_0 > \pm\sigma_0 = (2.254 \pm 0.051) \cdot 10^{-18} \ s^{-1} = (69.54 \pm 1.58) \frac{km}{s \cdot Mpc}.$$

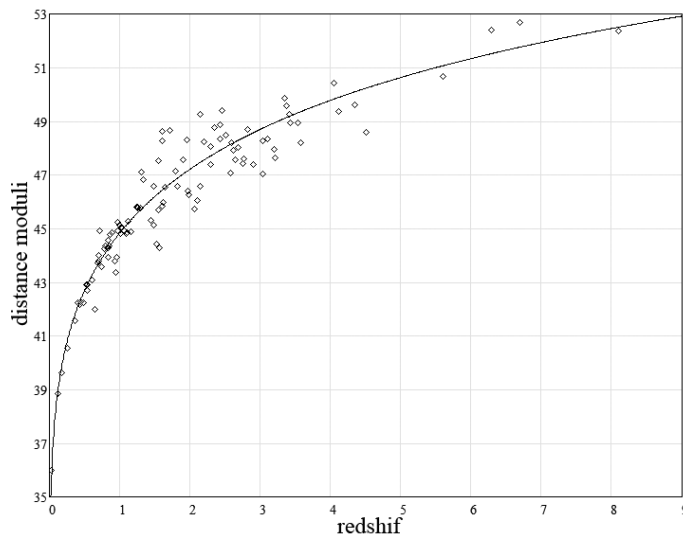Results of the best fitting are shown in Figs. 6, 7.

10

Figure 8: The theoretical Hubble diagram $\mu_0(z)$ of this model (solid); long GRBs observational data (109 points) are taken from Tables 1,2 of [17] and corrected for no time dilation.

If observations of long Gamma-Ray Bursts (GRBs) for small z are calibrated using SNe 1a, observational points are fitted with this theoretical Hubble diagram, too [4]. But for hard radiation of GRBs, the factor b may be smaller, and the real diagram for them may differ from the one for SNe 1a. With this limitation, the long GRBs observational data (109 points) are taken from Tables 1,2 of [17] and fitted in the same manner with $b = 2.137$. In this case we have: $< k > \pm\sigma_k = 43.262 \pm 8.447$ with $\chi^2 = 70.39$. By 108 degrees of freedom of this data set, it means that the hypothesis that $k(z) = const$ cannot be rejected with 99.81% C.L. For the Hubble constant we have in this case:

$$< H_0 > \pm\sigma_0 = (2.162 \pm 0.274) \cdot 10^{-18} \ s^{-1} = (66.71 \pm 8.45)\frac{km}{s \cdot Mpc}.$$

Results of the fitting are shown in Figs. 8,9.

Very recently, a new data set of 44 long Gamma-Ray Bursts was compiled with the redshift range of $[0.347; 9.4]$ [18], in which two empirical luminosity correlations (the Amati relation and Yonetoku relation) were used to calibrate observations. Because the GRB Hubble diagram calibrated using luminosity correlations is almost independent on the GRB spectra, as it has been shown by the authors, I use here values of $\mu(z_i) \pm \sigma_i$ from columns 7 of Tables 2 and 3 of [18], based on the Band function, but with both calibrations. If this data set is fitted in the same manner with $b = 2.137$, we have for the Amati calibration: $< k > \pm\sigma_k = 43.168 \pm 1.159$ with $\chi^2 = 40.585$. By 43 degrees of freedom of this data set, it means that the hypothesis that $k(z) = const$ cannot be rejected
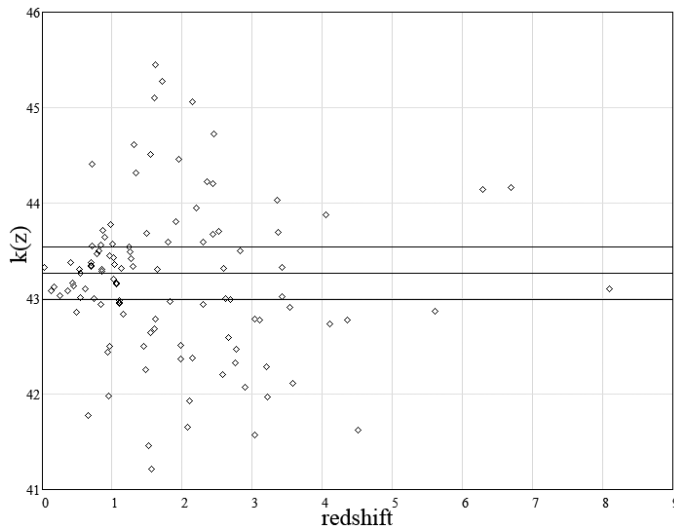
11

Figure 9: Values of $k(z)$ (109 points) and $< k(z) >$, $< k(z) > +\sigma_k$, $< k(z) > -\sigma_k$ (lines) for long GRBs.

with 57.66% C.L. For the Hubble constant we have in this case:

$$< H_0 > \pm\sigma_0 = (2.26 \pm 1.206) \cdot 10^{-18} \ s^{-1} = (69.732 \pm 37.226)\frac{km}{s \cdot Mpc}.$$

By $b = 2.137$, we have for the Yonetoku calibration: $< k > \pm\sigma_k = 43.148 \pm 1.197$ with $\chi^2 = 43.148$. It means that the hypothesis that $k(z) = const$ cannot be rejected with 46.5% C.L. For the Hubble constant we have in this case:

$$< H_0 > \pm\sigma_0 = (2.281 \pm 1.257) \cdot 10^{-18} \ s^{-1} = (70.386 \pm 38.793)\frac{km}{s \cdot Mpc}.$$

But best fitting values of b are less than 2.137 in both cases: $b = 1.885$ for the Amati calibration ($< k > \pm\sigma_k = 43.484 \pm 1.15$, $\chi^2 = 39.92$, with 60.57% C.L. and $< H_0 > \pm\sigma_0 = (1.954 \pm 1.035) \cdot 10^{-18} \ s^{-1} = (60.309 \pm 31.932)km/s/Mpc.$), and $b = 1.11$ for the Yonetoku one ($< k > \pm\sigma_k = 44.439 \pm 1.037$, $\chi^2 = 32.58$, with 87.62% C.L. and $< H_0 > \pm\sigma_0 = (1.259 \pm 0.601) \cdot 10^{-18} \ s^{-1} = (38.841 \pm 18.546)km/s/Mpc.$). Namely smaller values of this parameter for bigger photon energies are expected in the model. For best fitting values of b, values of distance moduli are overestimated in both calibrations: on ~ 0.225 for the Amati calibration, and on ~ 1.18 for the Yonetoku calibration, if we compare values of $< k >$ with its theoretical value of 43.259. It leads to the corresponding underestimation of the Hubble constant. Results of the best fitting for the Yonetoku calibration are shown in Fig. 10.

Recently, a new method to test cosmological models was introduced, based on the Hubble diagram for quasars [15]. The authors built a data set of 1,138
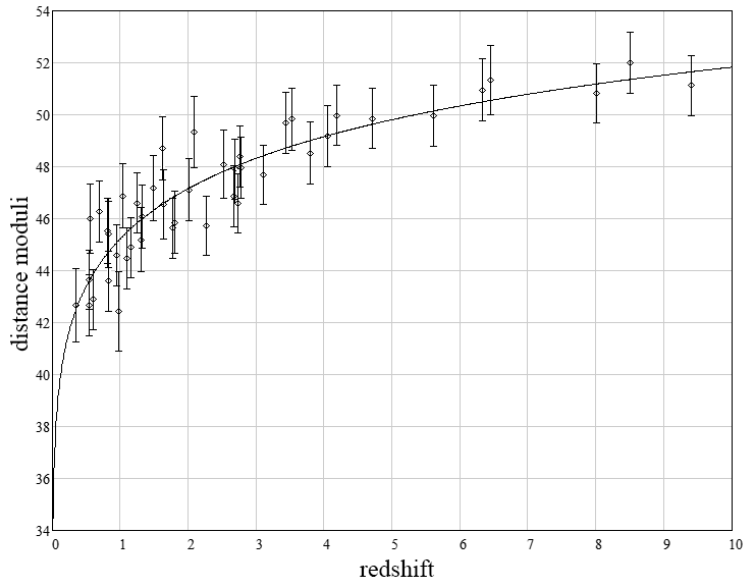
12

Figure 10: The theoretical Hubble diagram $\mu_0(z)$ of this model with $b = 1.11$ (solid); GRB observational data with the Yonetoku calibration (44 points) are taken from Table 3 of [18] and corrected for no time dilation.

quasars for this purpose. Some later, this method and the data set were used to compare different models [16]. I have used here the binned quasar data set (18 binned points) of the paper [16] to verify my model in the described above manner. This data set contains the sum of observed distance modulus and an arbitrary constant A. To find this unknown constant for the calibration of QSO observations, I have computed $< k'(z) >=< k(z) > +A$ and replaced $< k(z) >$ by its value for the JLA compilation; it gave: $A = 50.248$. This linking means that the average values of the Hubble constant should be identical for the two data sets. Subtracting this value of A, we get from the fitting of the quasar data by $b = 2.137$: $< k > \pm\sigma_k = 43.175 \pm 0.340$ with $\chi^2 = 23.378$. By 17 degrees of freedom of this data set, it means that the hypothesis that $k(z) = const$ cannot be rejected now with 13.73% C.L. For the Hubble constant we have:

$$< H_0 > \pm\sigma_0 = (2.253 \pm 0.340) \cdot 10^{-18} \ s^{-1} = (69.534 \pm 10.873)\frac{km}{s \cdot Mpc}.$$

Results of the fitting are shown in Fig. 11.

5.2 Comparison with the $LCDM$ cosmological model

To compare the above results of fitting with results for the $LCDM$ cosmology, let us replace $f_1(z) \rightarrow f_2(z)$ (see $Eq.$ 4) and repeat the calculations. Of course,

13

all data sets should remain now corrected for time dilation. The results of fitting are presented in Table 1; for convenience, the main above results for the model of low-energy quantum gravity are collected in the table, too. It is obvious, that confidence levels for both models do not allow to reject any of them.

the model of low-energy quantum gravity				
Data set	b	χ^2	C.L., %	$< H_0 > \pm\sigma_0$
SCP Union 2.1 [13]	2.137	239.635	100	68.22 ± 6.10
JLA [14]	2.365	30.71	43.03	69.54 ± 1.58
109 long GRBs [17]	2.137	70.39	99.81	66.71 ± 8.45
44 long GRBs [18],	2.137	40.585	57.66	69.73 ± 37.23
the Amati calibration	**1.885**	39.92	60.57	60.31 ± 31.93
44 long GRBs [18],	2.137	43.148	46.5	70.39 ± 38.79
the Yonetoku calibration	**1.11**	32.58	87.62	38.84 ± 18.55
quasars [16]	2.137	23.378	13.73	69.53 ± 10.87
the $LCDM$ cosmological model				
Data set	Ω_M	χ^2	C.L., %	$< H_0 > \pm\sigma_0$
SCP Union 2.1 [13]	0.30	217.954	100	69.68 ± 5.94
JLA [14]	0.30	29.548	48.90	70.08 ± 1.56
109 long GRBs [17]	0.30	66.457	99.94	70.04 ± 8.62
44 long GRBs [18],	0.30	40.777	56.81	68.99 ± 36.92
the Amati calibration	**0.49**	40.596	57.61	60.75 ± 32.44
44 long GRBs [18],	0.30	38.456	66.85	69.59 ± 36.10
the Yonetoku calibration	**1.0**	34.556	81.72	49.51 ± 24.35
quasars [16]	0.30	21.368	21.03	69.68 ± 10.42

Table 1: Results of fitting the Hubble diagram with the model of low-energy quantum gravity and the $LCDM$ cosmological model. The best fitting values of b and Ω_M for 44 long GRBs are marked by the bold typeface.

For me, it was a big surprise that the Einstein–de Sitter model ($Eq.$ 4 with $\Omega_M = 1$) cannot be rejected on a base of the full SCP Union 2.1 data set and the χ^2−criterion. We get $\chi^2 = 428.579$ and 99.9999% C.L. The cause is in a big number of small-z supernovae 1a in this set; it leads to a big number of degrees of freedom, but to small differences of χ^2 for models with similar values of $D_L(z)$ in this range of z. But if one splits the data set in two subsets, for example with $z \leq 0.5$ and $z > 0.5$, and uses the first subset to evaluate $< H_0 >$, then using this $< H_0 >$ and the second subset to compute χ^2 by much smaller number of degrees of freedom, one can reject this model with high probability (when $z > 0.5$, we get $\chi^2 = 247.551$ by 166 observations and 0.004% C.L.). Results for the model of low-energy quantum gravity and the $LCDM$ cosmological model are not essentially changed by the splitting. But the Einstein–de Sitter model with $\Omega_M = 1$ bests the $LCDM$ cosmological model with any amount of dark energy for the 44 long GRBs data set with the Yonetoku calibration.
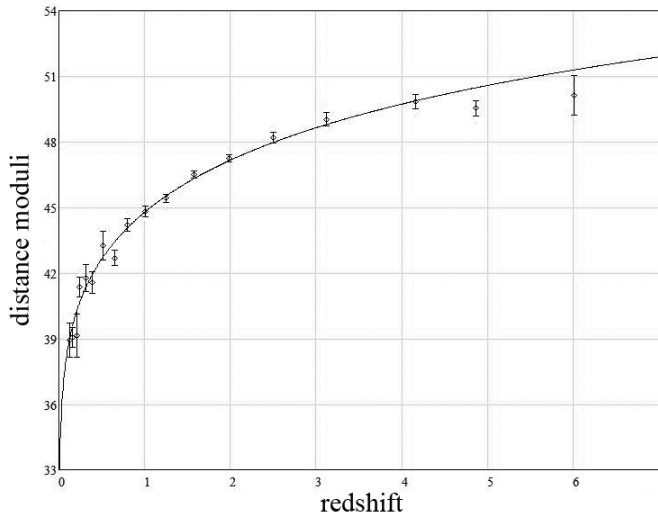
Figure 11: The theoretical Hubble diagram $\mu_0(z)$ of this model (solid); quasar observational data (18 binned points) [16] are corrected for no time dilation.

5.3 The Hubble parameter $H(z)$ of this model

If the geometrical distance is described by $Eq.$ 1, for a remote region of the universe we may introduce the Hubble parameter $H(z)$ in the following manner:

$$dz = H(z) \cdot \frac{dr}{c}, \tag{10}$$

to imitate the local Hubble law. Taking a derivative $\frac{dr}{dz}$, we get in this model for $H(z)$:

$$H(z) = H_0 \cdot (1 + z). \tag{11}$$

It means that in the model:

$$\frac{H(z)}{(1 + z)} = H_0. \tag{12}$$

The last formula gives us a possibility to evaluate the Hubble constant using observed values of the Hubble parameter $H(z)$. To do it, I use here 28 points of $H(z)$ from [19] and one point for $z < 0.1$ from [20]. The last point is the result of HST measurement of the Hubble constant obtained from observations of 256 low-z supernovae $1a$. Here I refer this point to the average redshift $z = 0.05$. Observed values of the ratio $H(z)/(1 + z)$ with $\pm \sigma$ error bars are shown in Fig. 12 (points). The weighted average value of the Hubble constant is calculated by the formula:

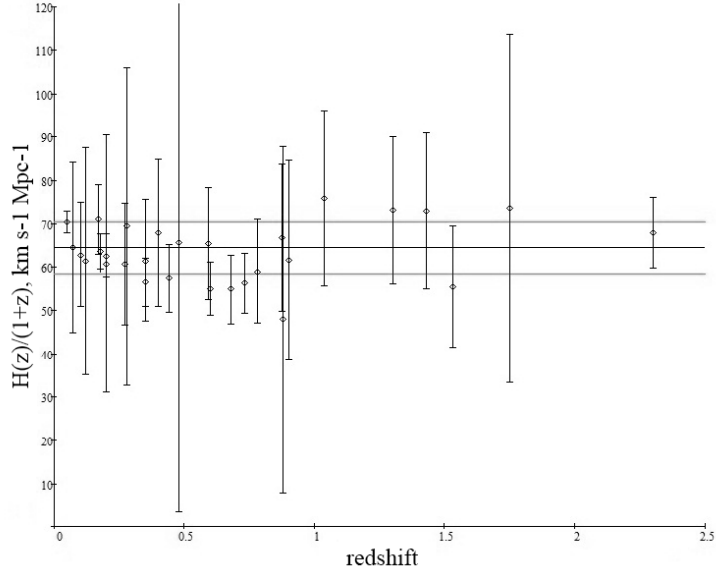$$< H_0 > = \frac{\sum \frac{H(z_i)}{1+z_i}/\sigma_i^2}{\sum 1/\sigma_i^2}. \tag{13}$$

15

Figure 12: The ratio $H(z)/(1 + z) \pm \sigma$ and the weighted value of the Hubble constant $< H_0 > \pm\sigma_0$ (horizontal lines). Observed values of the Hubble parameter $H(z)$ are taken from Table 1 of [19] and one point for $z < 0.1$ is taken from [20].

The weighted dispersion of the Hubble constant is found with the same weights:

$$\sigma_0^2 = \frac{\sum(\frac{H(z_i)}{1+z_i} - < H_0 >)^2/\sigma_i^2}{\sum 1/\sigma_i^2}. \tag{14}$$

Calculations give for these quantities:

$$< H_0 > \pm\sigma_0 = (64.40 \pm 5.95) \ km \ s^{-1} \ Mpc^{-1}. \tag{15}$$

The weighted average value of the Hubble constant with $\pm\sigma_0$ error bars are shown in Fig. 12 as horizontal lines.

Calculating the χ^2 value as:

$$\chi^2 = \sum \frac{(\frac{H(z_i)}{1+z_i} - < H_0 >)^2}{\sigma_i^2}, \tag{16}$$

we get $\chi^2 = 16.491$. By 28 degrees of freedom of our data set, it means that the hypothesis described by $Eq.$ 11 cannot be rejected with 95% C.L.

If we use another set of 21 cosmological model-independent measurements of H(z) based on the differential age method [21], we get (see Fig. 13):

$$< H_0 > \pm\sigma_0 = (63.37 \pm 4.56) \ km \ s^{-1} \ Mpc^{-1}. \tag{17}$$

16

The value of χ^2 in this case is smaller and equal to 3.948. By 21 degrees of freedom of this new data set, it means that the hypothesis described by *Eq. 11* cannot be rejected with 99.998% C.L.
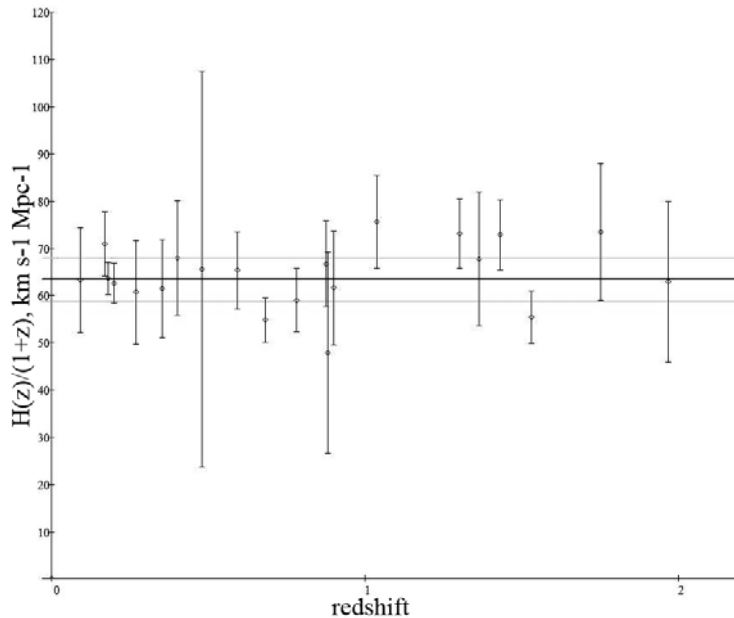

Figure 13: The ratio $H(z)/(1+z)\pm\sigma$ and the weighted value of the Hubble constant $<H_0>\pm\sigma_0$ (horizontal lines). Observed values of the Hubble parameter $H(z)$ are taken from [21].

Some authors try in a frame of models of expanding universe to find deceleration-acceleration transition redshifts using the same data set (for example, [19]). The above conclusion that the ratio $H(z)/(1+z)$ remains statistically constant in the available range of redshifts is model-independent. For the considered model, it is an additional fact against dark energy as an admissible alternative to the graviton background.

5.4 The Alcock-Paczynski test of this model

The Alcock-Paczynski cosmological test consists in an evaluation of the ratio of observed angular size to radial/redshift size [22]. Recently, this test has been carried out for a few cosmological models by Fulvio Melia and Martin Lopez-Corredoira [23]. They used new model-independent data on BAO peak positions from [24] and [25]. For two mean values of z ($<z>= 0.57$ and $<z>= 2.34$), the measured angular-diameter distance $d_A(z)$ and Hubble parameter $H(z)$ give for the observed characteristic ratio $y_{obs}(z)$ of this test the values: $y_{obs}(0.57) = 1.264 \pm 0.056$ and $y_{obs}(2.34) = 1.706 \pm 0.076$. In this model we have: $d_{com}(z) = d_A(z) = r(z)$, where $d_{com}(z)$ is the cosmological comoving

17

distance. Because the Universe is static here, the ratio $y(z)$ for this model is defined as:

$$y(z) = \frac{r(z)}{z \cdot \frac{d}{dz} r(z)} = \frac{r(z) \cdot H(z)}{cz} = (1 + \frac{1}{z}) \cdot \ln(1 + z), \qquad (18)$$

where $H(z)$ is defined by $Eq.$ 10. This function without free parameters characterizes any tired light model (model 6 in [23]). We have only two observational points to fit them with this function. Calculating the χ^2 value as:

$$\chi^2 = \sum \frac{(y_{obs}(z_i) - y(z_i))^2}{\sigma_i^2}, \qquad (19)$$

we get $\chi^2 = 0.189$, that corresponds to the confidence level of 91% for two degrees of freedom.

6 Conclusion

As it is shown above, the Hubble diagram of supernovae 1a, GRBs and quasars being corrected for no time dilation, the Hubble parameter $H(z)$ and the ratio of observed angular size to radial/redshift size are well fitted in this model. The Hubble diagram for GRBs may differ in the model from the diagram for SNe 1a, and some signs of this difference are seen, perhaps, in the case of the 44 long GRBs data set. In the model, space-time is flat, and the geometrical distance as a function of the redshift coincides with the angular diameter distance. Given that a galaxy number density is constant in the no-evolution scenario, theoretical predictions for galaxy number counts in this model have been found using only the luminosity and geometrical distances defined by $Eqs.1, 2$ [26]. The geometrical distance $r(z)$ of this model is very different from the one of the standard model; for example, GRB 090429B with $z = 9.4$ [27] took place 24.6 Gyr ago in a frame of this model; the age of the Universe of the standard model: $\sim 13.5\ Gyr$ corrseponds here to $z \simeq 2.6$.

At present this model is not a full cosmological one; it is necessary to develop many open problems to bring it closer to the pursuable completeness. But even now it has interesting advantages: the model's parameters H_0 and b are computable; there is not any need in dark energy (and in the Bing Bang, inflation, expansion).

I am grateful to the authors of the paper [16] for the binned quasar data set which I have received by my request.

References

[1] Pikovski, I. et al. *Nature Physics* 2012, *8, 393.*

[2] Bekenstein, J. D. [arXiv:1211.3816 [gr-qc]].

[3] Ivanov, M.A. In the book "Focus on Quantum Gravity Research", Ed. D.C. Moore, Nova Science, NY - 2006 - pp. 89-120; [hep-th/0506189], [http://ivanovma.narod.ru/nova04.pdf].

[4] Ivanov, M.A. Selected papers on low-energy quantum gravity. [http://ivanovma.narod.ru/selected-papers-Ivanov11.pdf].

[5] Ivanov, M.A. [astro-ph/0609518].

[6] Anderson, J.D. et al. *Phys. Rev. Lett.* 1998, *81,* 2858; *Phys. Rev.* 2002, *D65,* 082004; [gr-qc/0104064 v4].

[7] Ivanov, M.A. In the Proceedings of 14th Workshop on General Relativity and Gravitation (JGRG14), Nov 29 - Dec 3 2004, Kyoto, Japan; [gr-qc/0410076].

[8] Abbott, B.P. et al. [arXiv:1602.03838 [gr-qc]].

[9] Turyshev, S. et al. *Phys. Rev. Lett.* 2012, *108,* 241101; [arXiv:1204.2507 [gr-qc]].

[10] Famaey, B. and McGaugh, S. [arXiv:1112.3960v2 [astro-ph.CO]].

[11] Milgrom, M. *ApJ,* 1983, *270,* 365370 and 371383.

[12] Riess, A.G. et al. *ApJ,* 2004, *607,* 665; [astro-ph/0402512].

[13] Suzuki, N. et al. *ApJ,* 2012, *746,* 85; [arXiv:1105.3470v1 [astro-ph.CO]].

[14] Betoule, M. et al. [arXiv:1401.4064v2 [astro-ph.CO]].

[15] Risaliti, G. and Lusso, E. *ApJ,* 2015, *815,* 33; [arXiv:1505.07118 [astro-ph.CO]].

[16] Lopez-Corredoira, M., Melia, F., Lusso, E. and Risaliti, G. [arXiv:1602.06743 [astro-ph.CO]].

[17] Wei, H. [arXiv:1004.4951v3 [astro-ph.CO]].

[18] Lin, H.-N., Li, X., and Chang, Z. [arXiv:1604.02285 [astro-ph.HE]].

[19] Farooq, O., and Ratra, B. [arXiv:1301.5243].

[20] Riess, A. G., et al., *ApJ* 2011, *730,* 119.

[21] Moresco, M. [arXiv:1503.01116v1 [astro-ph.CO]].

[22] Alcock, C. and Paczynski, B., *Nature* 1979, *281,* 358.

[23] Melia, F., and Lopez-Corredoira, M. [arXiv:1503.05052v1 [astro-ph.CO]].

[24] Anderson, L. et al., MNRAS 2014, *441*, 24.

[25] Delubac, T. et al., *AA* 2015, *574*, A59.

[26] Ivanov, M.A. [astro-ph/0606223v3].

[27] Cucchiara, A. et al. *ApJ* 2011, *736*, 7.